Journal of the Oceanographical Society of Japan
Vol. 33, pp. 137 to 150, 1977

Field Data Support of Three-seconds Power Law and $gu_*\sigma^{-4}$-spectral Form for Growing Wind Waves*

Sanshiro KAWAI**, Kozo OKADA*** and Yoshiaki TOBA**

Abstract: Observational data on air-sea boundary processes at the Shirahama Oceanographic Tower Station, Kyoto University, obtained in November, 1969, was analyzed and presented as an example representing the structure of growing wind-wave field. The condition was an ideal onshore wind, and the data contained continuous records of the wind speed at four heights, the wind direction, the air and water temperatures, the tides, and the growing wind waves, for more than six hours. The main results are as follows. Firstly, in both of the wind speed and the sea surface wind stress, rather conspicuous variations of about six-minute period were appreciable. Secondly, the three-seconds power law and its lemma expressed by $H^*=BT^{*3/2}$ and $\delta=2\pi BT^{*-1/2}$, respectively, are very well supported by the data, where $H^*(\equiv gH/u_*^2)$ and $T^*(\equiv gT/u_*)$ are the dimensionless significant wave height and period, respectively, δ the wave steepness, u_* the friction velocity of air, g the acceleration of gravity, and $B=0.062$ is a universal constant. Thirdly, the spectral form for the high-frequency side of the spectral maximum is well expressed by the form of $\phi(\sigma)=\alpha_s g u_* \sigma^{-4}$, where σ is the angular frequency and $\phi(\sigma)$ the spectral density. The value of α_s is determined as 0.062 ± 0.010 from the observational data. There is a conspicuous discrepancy between the spectral shape of wind waves obtained in wind-wave tunnels and those in the sea, the former containing well-defined higher harmonics of the spectral peak, and consequently there is an apparent difference in the values of α_s also. However, it is shown that the discrepancy of α_s may be eliminated by evaluating properly the energy level of the spectral form containing higher harmonics.

1. Introduction

Studies on the growth of wind waves have experienced remarkable developments up to the present, since SVERDRUP and MUNK (1947) first introduced the concept of significant waves as an idealization of the complex state of wind waves, and treated the problem based on an energetic consideration and empirical facts. They succeeded to a certain extent in predicting the growth of wind waves. PIERSON (1952) and other investigators introduced another treatment of irregular wind waves by means of energy spectrum, although the concept of energy spectrum is also an idealization as was pointed out by TOBA *et al.* (1975). Since then many observational data of wave spectra have been accumulated, and some standard forms of the spectra, including two-dimensional spectra, have been proposed empirically, for example, by PIERSON and MOSKOWITZ (1964), HASSELMANN *et al.* (1973), MITSUYASU (1973), and MITSUYASU *et al.* (1975). For the essential part of the one-dimensional spectra for high frequency side of the spectral peak, they assumed the form proportional to $g^2\sigma^{-5}$, since PHILLIPS (1958) proposed the $g^2\sigma^{-5}$-form on the basis of a dimensional considerations, where g is the acceleration of gravity and σ the angular frequency.

In recent years, one of the authors treated macroscopic structure of the growing wind-wave field from dimensional considerations, and proposed some functional relations, such as the three-seconds power law between the dimensionless wave height and period of significant waves, and a relation between the wave steepness and dimensionless wave period (TOBA, 1972, 1973, 1974). Also, combining the three-seconds power

* Received Aug. 30, 1976, revised Feb. 23 and accepted Mar. 23, 1977.

** Geophysical Institute, Faculty of Science, Tohoku University, Sendai 980, Japan

*** Present address: Tohoku Center, Japan Weather Association, Sendai 980, Japan

law with the concept of similarity of wind-wave spectra, he proposed a $gu_*\sigma^{-4}$-form for wave spectra (TOBA, 1973a). These proposed relations, especially the spectral form, were supported mainly by his data from wind-wave tunnel experiments. In the present article, we will present a strong support to these relations and the spectral form, on the basis of field data obtained at the Shirahama Oceanographic Tower Station of Kyoto University in a former year.

The outline of the observation and some preliminary results of the analysis were reported by TOBA *et al.* (1971). However, a short description of the conditions of observation is given below in the present section, especially concerning the fields of wind and wind waves, although the observational project was more extensive including those of breaking waves and sea-salt particles.

The oceanographic tower station is located at the mouth of Tanabe Bay, Wakayama prefecture, as shown in Fig. 1. The tower is made of steel angles, with a small instrumentation room at the height from 6.8 m to 9.0 m and a working floor at the level of 4.5 m above the mean sea level, the total height of the tower being 13 meters above the mean sea level. The observation for the present analysis was performed in the period from November 3 to 10, 1969. This period was selected expecting the out-burst of the winter monsoon, whose direction was northwest (onshore), affording a fairly long fetch of the sea to the tower station. The anemometers and the wave gauge were

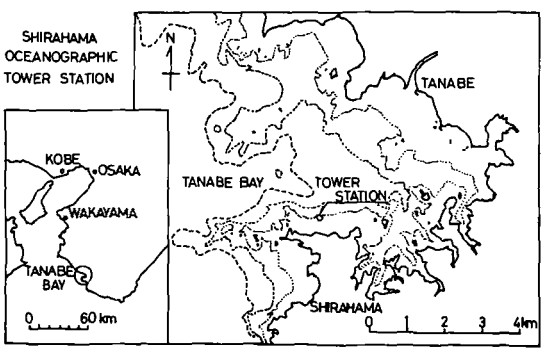

Fig. 1. The location of the Shirahama Oceanographic Tower Station (cited from HAYAMI *et al.*, 1964).

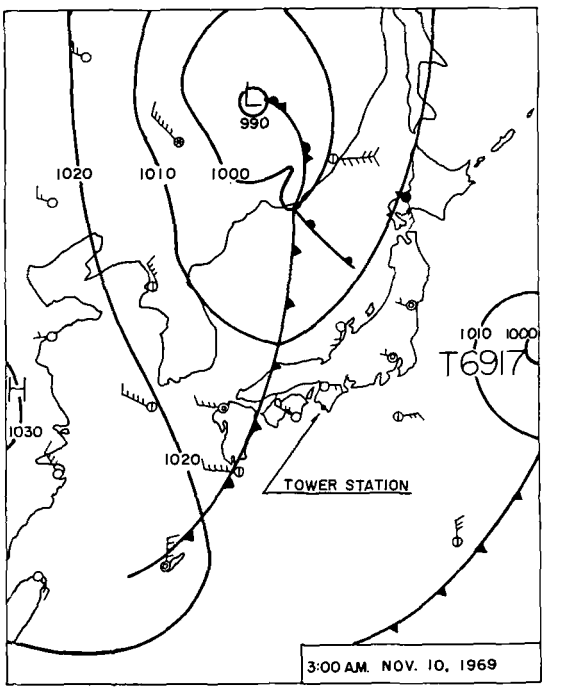

Fig. 2. Weather map at about 6 hours before the start of the continuous observation.

Table 1. Main items of observation and instruments used.

Item	Sensor	Remarks
Wind speed	Small 3-cup anemometer with a photo-electric device	Nominal heights: 13 m, 6 m, 3 m and 1.5 m
Wind direction	Wind vane	Nominal height: 10 m
Surface elevation	Capacitance-wire type wave gauge manufactured by Denshikogyo Co., Ltd., type VM-105. Diameter of sensor 1 mm	
Breaking of waves	Visual marker on wave records	At the site of wave gauge
Air temperature	Thermister	Nominal height: 6 m
Sea surface temperature	Thermister	Mounted on a small float
Sea level	Pressure-type tide gauge	Nominal depth: 3 m

Table 2. Main characteristic values for the continuous 26 runs of the observation.

Run no.	Time	15-min average wind speed U_{10} (m s^{-1})	Friction velocity u_* (cm s^{-1})	Wind direction	Significant wave H (cm)	Significant wave T (s)	Spectral peak frequency f_m (s^{-1})	Air temp. (°C)	Water temp. (°C)
1	09:50-10:00	7.0	48.0	WSW	17.0	2.4	—	18.3	21.9
2	10:00-10:15	6.9	34.2	WSW	15.3	1.5	—	18.7	21.9
3	10:15-10:30	6.5	28.9	WSW	12.7	1.3	—	18.8	21.9
4	10:30-10:45	6.3	30.6	WSW	13.8	1.3	—	18.8	21.9
5	10:45-11:00	6.5	28.2	WSW	16.7	1.5	—	18.9	21.9
6	11:00-11:15	6.8	26.3	WSW	16.8	1.7	0.45	19.0	21.9
7	11:15-11:30	6.4	19.1	WSW	16.1	1.5	0.50	18.9	21.9
8	11:30-11:45	7.0	24.0	WSW	21.4	1.9	0.375	18.8	21.9
9	11:45-12:00	7.3	35.8	WNW	21.8	1.6	0.35	18.0	21.9
10	12:00-12:15	6.5	30.6	WNW	25.4	1.8	0.40	18.0	21.9
11	12:15-12:30	5.9	27.8	WNW	25.9	1.9	0.35	18.0	21.9
12	12:30-12:45	4.8	23.4	WNW	23.8	1.9	0.35	18.1	21.9
13	12:45-13:00	4.9	22.7	WNW	25.3	1.8	0.30	18.2	21.9
14	13:00-13:15	5.8	25.5	WNW	26.1	2.0	0.30	18.2	21.9
15	13:15-13:30	7.1	32.8	WNW	31.3	2.0	0.35	18.0	21.9
16	13:30-13:45	6.8	31.0	WNW	29.6	2.0	0.30	17.8	21.9
17	13:45-14:00	7.9	33.3	WNW	33.9	2.1	0.35	17.7	21.9
18	14:00-14:15	8.8	37.2	NW	35.3	2.1	0.35	17.3	21.9
19	14:15-14:30	9.4	37.6	NW	34.5	2.1	0.30	16.8	21.9
20	14:30-14:45	11.3	45.4	NW	42.9	2.2	0.35	16.2	21.8
21	14:45-15:00	10.9	49.5	NW	54.4	2.4	0.40	15.9	21.8
22	15:00-15:15	10.3	46.2	NW	48.1	2.2	0.30	15.8	21.8
23	15:15-15:30	10.6	47.0	NNW	44.0	2.3	0.275	15.5	21.8
24	15:30-15:45	10.9	50.3	NNW	47.5	2.2	0.30	15.2	21.9
25	15:45-16:00	10.5	44.9	NNW	51.9	2.2	0.25	15.0	21.9
26	16:00-16:15	12.0	52.5	NNW	54.9	2.4	0.30	14.9	21.9

mounted on steel pipes, and projected out about 1 meter to the west from the angle of the northwest corner of the tower, in order to avoid the influence of the body of the tower to the natural conditions. The items of the observation and instruments used are shown in Table 1.

On November 10, a few minutes past nine in the morning, a cold front, which is shown in Fig. 2, passed through the site, and the winter monsoon began to blow the sea surface, which had been very smooth but somewhat undulated with gentle swells. As the wind continued to blow, the wind waves grew up on and on. We were able to take records of this process for more than 6 hours continuously, until it became too dark to work securely at the sea. When we gave up continuing the observation, the wind speed was greater than 12 m s^{-1}, and the wave height was so high, almost exceeding the sensing limit of the wave gauge of 1.5 m. The continuous record was divided into 26 runs of 15 minutes each. In Table 2 are shown for each run the mean wind speed at 10-m level U_{10}, the friction velocity of air u_* which was determined from the wind profiles, the wind direction, the significant wave height H and the significant wave period T which were obtained by the peak-to-peak method, the frequency f_m of the spectral peak, the air temperature, and the sea surface temperature. It should be noted that the peak-to-peak method was adopted in defining the significant waves because the existence of swell makes it difficult to use the zero-up-cross method, especially in the earlier runs.

2. The variation of wind and wind stress

The profiles of wind speed averaged for each 15 minutes are shown in Fig. 3. From Run 1

to Run 8, which are shown in the upper part (a), the points of the top anemometer deviate apparently from the logarithmic profiles. During these runs the wind direction was WSW. In that direction, a small peninsula and a few tiny islands exist within about 1 km from the tower station, as shown in Fig. 1. It is considered that by these obstacles the thickness of the atmospheric boundary layer on the sea surface became thin, and the top anemometer was out of the layer; or otherwise, some organized eddies produced by the obstacles caused the deviation of the wind profile from the logarithmic ones. These phenomena were also observed in August, 1968 at the same site, and reported by TOBA *et al.* (1971). Consequently, the data of the top anemometer from Run 1 to Run 8 is excluded in the following analysis.

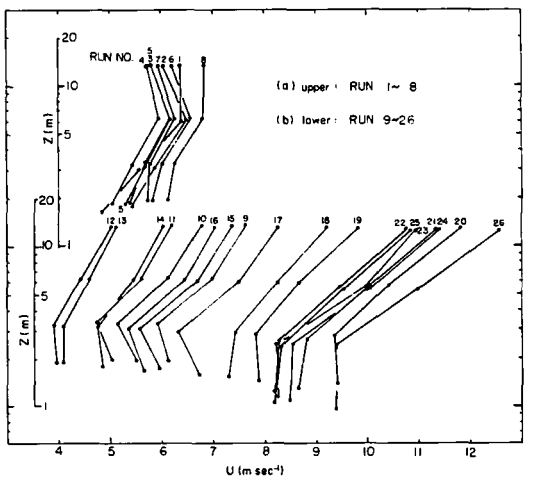

Fig. 3. Wind profiles of 26 runs.

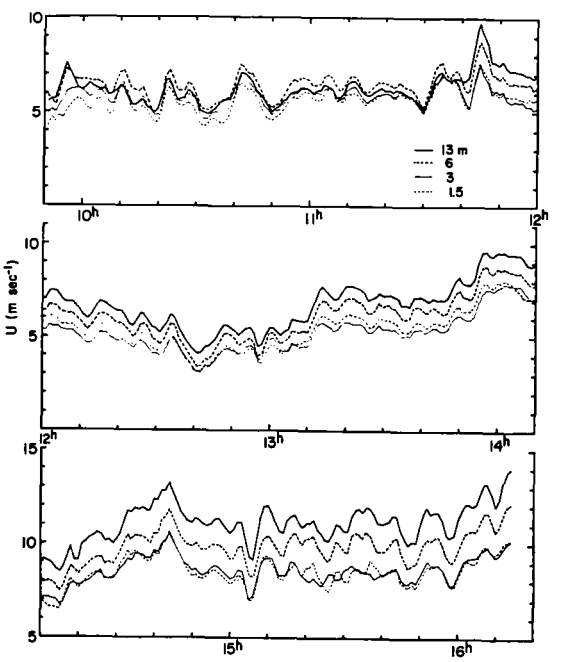

Fig. 4. Variation of one-minute average wind speed.

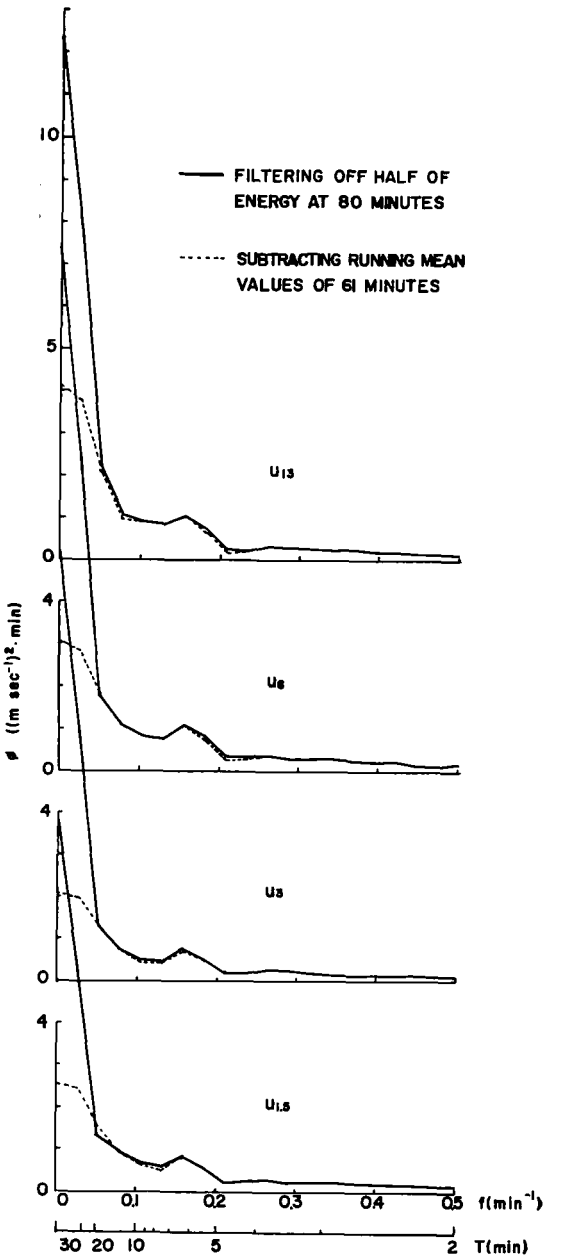

Fig. 5. Power spectra of wind speed computed after filtering off the long period power by use of two kinds of high-pass filters.

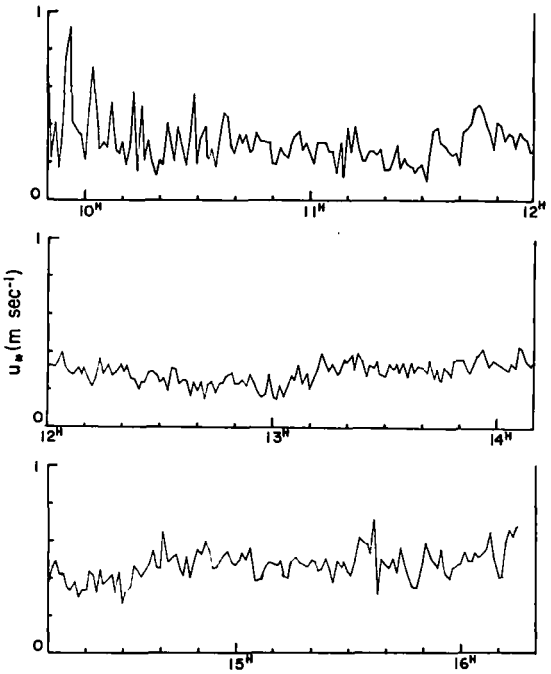

Fig. 6. Variation of friction velocity.

Concerning the rest of the runs, the wind profiles did not necessarily fit well the logarithmic or near-logarithmic profiles. However, the points of all of the four heights have been used in the analysis, since the cause of the peculiar shapes of the profiles is not conceived and these data are considered equally significant.

In Fig. 4 is shown the variation of 1-minute average wind speed of the four heights throughout the observation. The small cup anemometers used were well responsible for 1-minute variation of wind speed. It is noted from the figure that there was a periodic variation of the wind speeds, the period being about 6 minutes. The period of about 6 minutes is also appreciable by the peak of the power spectra shown in Fig. 5. The power spectra have been computed after filtering off the long period power by two kinds of high-pass filters. The first one cuts off a half of power at a period of 80 minutes, and the results are shown by solid lines. In the second one the running-mean values of 61 minutes are subtracted, and the results are shown by dashed lines. It is remarkable that the periodic variations are seen at all heights, and that they are fairly well-correlated with each other. Consequently, it should be concluded that this variation is

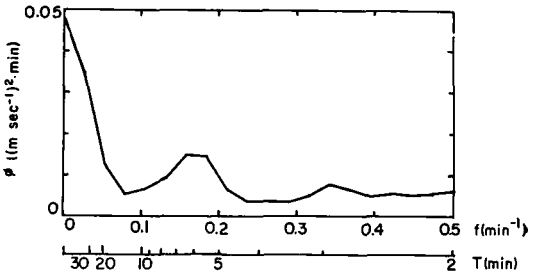

Fig. 7. Power spectrum of friction velocity. The filter used is one filtering off half of power at 80 minutes.

real. The values of the wind stress have been computed by the method of least squares assuming the logarithmic profiles, by use of the data of three (Runs 1 through 8) or four heights (Runs 9 through 26). In Fig. 6 is shown the variation of the computed friction velocity u_*. It is seen that the wind stress also shows a variation of about 6-minute period. In Fig. 7 is shown its power spectrum. The spectrum has been computed after filtering off the long period power by the first type of the high-pass filter used in the wind speed. The peak at about 6 minutes is dominant.

If we use the conventional 10-minute average values for the wind speed, we could not find such a kind of periodicity. Although we do not conceive the cause of the periodicity at present, it should be kept in mind for future investigation that the growth of wind waves proceeds under the conditions of such a kind of complicated fine structure of the wind blowing over the sea.

3. Significant waves and the three-seconds power law

Studiess on the growth of wind waves, by means of significant waves as the representation of wind-wave field, were undertaken by many investigators since SVERDRUP and MUNK (1947). The results have practically been used for the prediction of wind waves as, for example, the SMB method. One of the present authours (TOBA, 1972, 1973) proposed a universal relation between the dimensionless significant wave height and period as the three-seconds power law:

$$H^*=BT^{*3/2},\ B=0.062 \qquad (1)$$

and also its lemmas

$$u_0=\pi^3B^2u_* \qquad (2)$$

and

$$\delta=2\pi BT^{*-1/2} \qquad (3)$$

where $H^*=gH/u_*^2$, $T^*=gT/u_*$, $\delta=H/L$; H, T and L are the wave height, the period and the wave length of significant waves, respectively, g the acceleration of gravity, and u_0 the wave current, or the mass transport velocity by waves at the sea surface. The value of B as a universal constant was given empirically by use of his wind-wave tunnel data and empirical formulas by WILSON (1965) and MITSUYASU *et al.* (1971). He derived the relations also through a second procedure, and got the value of $B=(2\pi)^{-3/2}=0.0635$ (TOBA, 1974). In our observation we haven't any direct information of u_0, and we cannot verify the relation (2) by the measured data. However, it is shown below that the other two relations are very well supported by the present field data.

In Fig. 8 is shown the first relation. In the figure, the solid line shows (1) with the constant $B=0.062$. Solid circles show the present field data obtained from Table 1 excluding Run nos. 1 through 6, which included swells as will be shown in the succeeding section, and solid circles with a stem atop show the data including swells of Run nos. 1 through 6. Solid inverse triangles show the wind-wave tunnel data from TOBA (1972). Open circles show the values computed by eliminating gF/U_{10}^2 from the following formulas proposed by WILSON (1965):

$$\frac{gH}{U_{10}^2}=0.30\left[1-\left\{1+0.004\left(\frac{gF}{U_{10}^2}\right)^{1/2}\right\}^{-2}\right] \qquad (4)$$

and

$$\frac{gT}{2\pi U_{10}}=1.37\left[1-\left\{1+0.008\left(\frac{gF}{U_{10}^2}\right)^{1/3}\right\}^{-5}\right] \qquad (5)$$

where F is the fetch, and U_{10} the wind speed at the 10-m level. Open triangles show the values computed in the same way from the formulas proposed by MITSUYASU *et al.* (1971):

$$\frac{gH}{U_{10}^2}=2.15\times10^{-3}\left(\frac{gF}{U_{10}^2}\right)^{0.504} \qquad (6)$$

and

$$\frac{gT}{2\pi U_{10}}=5.07\times10^{-2}\left(\frac{gF}{U_{10}^2}\right)^{0.330} \qquad (7)$$

In the computation of the values of H^* and T^* from these formulas (4) and (5), and (6) and (7), an approximate value of $(C_D)^{1/2}$ of 0.040 has been used where C_D is the drag coefficient for the sea surface wind stress. Open squares show the relation

$$H^*=0.061\ T^{*3.03/2} \qquad (8)$$

which is the converted form, given by TOBA (1976), from the formulas proposed by HASSELMANN *et al.* (1973),

$$\frac{g^2E}{U_{10}^4}=1.6\times10^{-7}\frac{gF}{U_{10}^2} \quad \left(\text{for } \frac{gF}{U_{10}^2}\lesssim10^{-4}\right) \qquad (9)$$

and

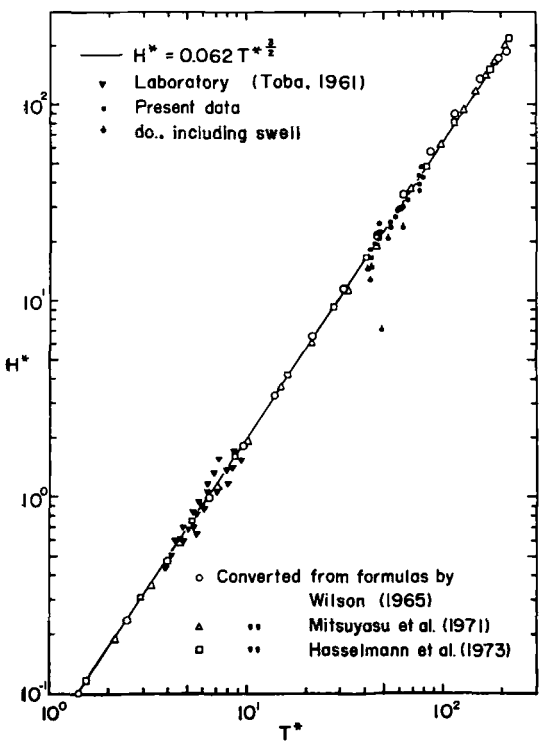

Fig. 8. Support of the three-seconds power law by various data.

$$\frac{U_{10}f_m}{g}=3.5\left(\frac{gF}{U_{10}^2}\right)^{-0.33} \quad \left(\text{for } \frac{gF}{U_{10}^2}\lesssim 10^{-4}\right) \qquad (10)$$

where E is the total energy of wind waves and f_m the frequency of the spectral maximum. Fig. 8 includes almost full range of H^* and T^* for wind waves, and we may conclude that the three-seconds power law is very universal, although the data including swells deviates.

In Fig. 9 is shown the relation (3). The meaning of symbols is the same as in Fig. 8. As is seen from the figure, the functional relation (3) between the wave steepness δ and T^*, or the wave age β, is very consistent between the wind-wave tunnel data and the present field data except for the data including swells. It should be noted here that when the zero-up-cross method is used for defining the significant waves, somewhat smaller value of B in (1) should be taken for the later runs of the observation. The change of the value of B depending on the definition of the significant waves contains some complicated problems, which are left as a problem to be solved in the future.

Since the definition of the significant waves has some indefiniteness as mentioned above, TOBA (1976) converted the relation (1) to the relation between the total energy E and the frequency f_m of the spectral maximum,

$$E^*=B_f f_m{}^{*-3},\ B_f=2.1\times10^{-4} \qquad (11)$$

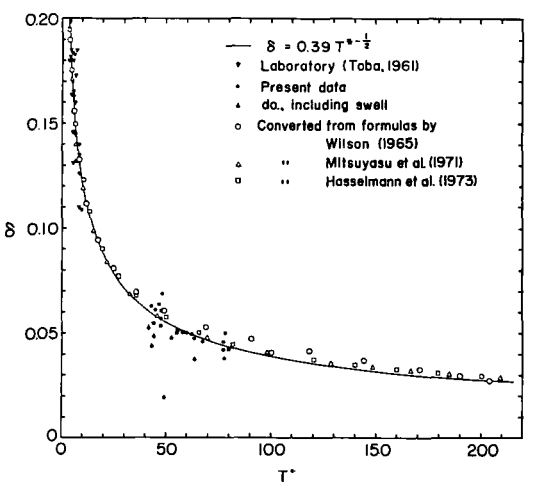

Fig. 9. Support of the relation of the wave steepness δ with T^*, or the wave age.

where $E^*=g^2E/u_*{}^4$ and $f_m{}^*=u_*f_m/g$. In the conversion, he used two relations among the quantities of spectrum and those of significant waves, namely,

$$f_m=(1.05T)^{-1} \qquad (12)$$

after MITSUYASU (1968) and TOBA (1973a), and

$$E=H^2/16 \qquad (13)$$

after LONGUET-HIGGINS (1952). Approximately the same relations as (11) are derived from original empirical relations proposed by MITSUYASU (1968, 1971):

$$\frac{g\sqrt{E}}{u_*{}^2}=1.31\times10^{-2}\left(\frac{gF}{u_*{}^2}\right)^{0.504} \qquad (14)$$

and

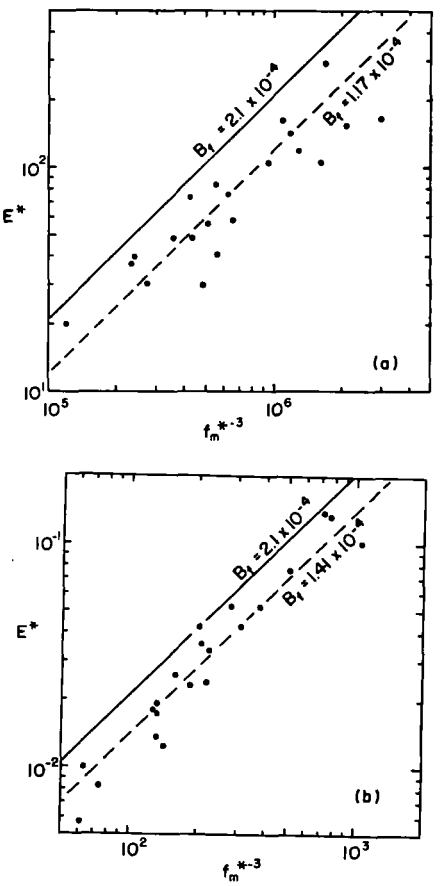

Fig. 10. Minus-third power law, (a) the present field observation, (b) Toba-Pierson wind-wave tunnel data (TOBA, 1973).

$$\frac{u_* f_m}{g}=1.00\left(\frac{gF}{u_*^2}\right)^{-0.330} \qquad (15)$$

from which

$$E^*=1.72\times10^{-4}f_m{}^{*-3.05} \qquad (16)$$

is derived. From (9) and (10), we may also obtain

$$E^*=2.0\times10^{-4}f_m{}^{*-3.03} \qquad (17)$$

In this conversion, the value of $C_D=1.0\times10^{-3}$, which was used by HASSELMANN *et al.* (1973), has been used.

In Fig. 10(a) is shown the relation (11) for our field data and in Fig. 10(b) for Toba-Pierson wind-wave tunnel data (see TOBA, 1973). The method for the computation of the spectral values for the present field data will be explained in the next section. In both of the two figures, at least the statistical proportionality of E^* to $f_m{}^{*-3}$ is evident, but the coefficient of proportion is

$$B_f=(1.17\pm0.37)\times10^{-4} \qquad (18)$$

for (a) and

$$B_f=(1.41\pm0.33)\times10^{-4} \qquad (19)$$

for (b), and these values are somewhat different from the value given by (11). The discrepancy is explained mainly by the fact that the relation (12) and (13) are not always satisfied by these observational data. For our field data,

$$f_m T=0.683\pm0.093 \qquad (20)$$

and

$$E/(H^2/16)=1.67\pm0.39 \qquad (21)$$

and these values are ordinary values as observed in the sea, as discussed by IWATA *et al.* (1970, 1971). For the wind-wave tunnel data, the relation (12) is satisfied, but the relation (13) is not, and for those data

$$E/(H^2/16)=0.785\pm0.231 \qquad (22)$$

At this point, it should be noted that the significant wave height H for those data was presented by use of the relation $H=1.6\bar{H}$ after LONGUET-HIGGINS (1952), where $\bar{H}$ was the average wave height, which was given as the original data by TOBA (1972). In Fig. 9, very high values of δ for the wind-wave tunnel data, shown by inverse solid triangles for small T^*, stem from this fact. It should also be noted that the inverse solid triangles plotted in Figs. 8 and 9 also represent those values of H. The delicate problem of the value of numerical factors included in the above equations is yet to be investigated.

4. Spectral form

It is well known that the energy spectrum of growing wind waves has a conspicuous peak and the spectral form of the high-frequency side of the spectral maximum is expressed by a negative power law. PHILLIPS (1958) proposed, on the basis of a dimensional consideration, the existence of an equilibrium range expressed by

$$\phi(\sigma)=\alpha_p g^2\sigma^{-5} \qquad (23)$$

where α_p is a constant. Since then much observational data has been accumulated, and at present it is recognized at least that α_p is not a constant but depends on other factors, such as u_*, which was neglected in the Phillips' analysis.

On the other hand, TOBA (1973a; partly revised in TOBA, 1974a) combined the three-seconds power law shown in (1) with the concept of similarity of the wind-wave spectra, and proposed the $gu_*\sigma^{-4}$-form. It is expressed by

$$\phi(\sigma)=\alpha_s g_* u_* \sigma^{-4},\ g_*\equiv g+\frac{S\kappa^2}{\rho_w} \qquad (24)$$

where S is the surface tension, κ the wave number, ρ_w the density of water, and the constant α_s was given empirically as 0.020 from his wind-wave tunnel data. For gravity wave range the second term in g_* is neglected, and g_* may be replaced by g.

Both of the formulas (23) and (24) are the negative power law, and are expressed by the general form

$$\phi(\sigma)=\alpha\sigma^{-m} \qquad (25)$$

where m is 5 for (23) and 4 for (24), and α is a constant for (23) and depends linearly on u_* for (24). In comparing our observational data

with the general form (25), two sets of wave data series were used. The first set, or Series A, is composed of data sampled in nearly central 1.5 minutes of each run. However, the data from Run 1 to Run 5 were excluded, for in these runs wind waves were not superior relative to swells, and wind-wave spectra were submerged in the spectra of swells. The second set, or Series B, is composed of 28 runs of 3-minute records sampled continuously from Run 13 to Run 15 of Series A. The total length of the 28 runs is 30 minutes, and each run is overlapped by 2 minutes with the succeeding run. In both series, the data has been digitized every 0.1 second. The degree of freedom in computing spectra was 18 for Series A and 36 for Series B. At the part of straight line in $\log\phi$-$\log\sigma$ plots for each spectral data, the method of least squares was used for the determination of m and $\log\alpha$, or α in the formula

$$\log\phi=-m\log\sigma+\log\alpha \qquad (26)$$

which is the logarithmic version of the formula (25).

The value of m computed for each run is shown in Column 4 of Table 3 for Series A, and in Column 3 of Table 4 for Series B. The range of frequency used in the least-square processing was decided visually on the $\log\phi$-$\log\sigma$ plots, and is shown in Column 3 of Table 3 for Series A. For Series B the range was from 0.55 to 3 Hz, equally for 28 runs. The mean value of m with its standard deviation is

$$m=4.15\pm0.25 \qquad (27)$$

for Series A and

$$m=4.11\pm0.13 \qquad (28)$$

for Series B. These values show that the formula (24) is reasonable but the formula (23) does not correspond to our observational data.

Based on these results, values of α have been

Table 3. Characteristic values of spectra for Series A.

1	2	3	4	5	6
Run no.	Time of beginning	Range (Hz)	m	α (10^3 cm^{2}s)	α_s (10^{-2})
6	11:06	1.0 -3.0	4.27	1.41	5.47
7	11:21	.5 -3.0	4.09	1.28	6.81
8	11:36	.4 -3.0	3.98	1.32	5.61
9	11:51	.7 -2.0	4.46	1.81	5.15
10	12:06	.4 -2.5	4.23	1.19	3.96
11	12:21	.4 -2.5	4.13	1.53	5.63
12	12:36	.35-2.5	4.05	1.57	6.84
13	12:52	.55-3.0	4.35	1.24	5.57
14	13:07	.4 -2.5	3.59	1.62	6.48
15	13:20	.4 -2.4	3.95	1.90	5.91
16	13:36	.35-1.5	3.97	2.16	7.10
17	13:51	.45-2.5	4.41	1.94	5.94
18	14:06	.35-2.5	4.16	2.28	6.25
19	14:21	.5 -2.4	4.36	3.02	8.18
20	14:36	.4 -1.5	4.23	3.29	7.40
21	14:51	.4 -3.0	4.06	2.54	5.23
22	15:02	.45-2.0	4.67	2.94	6.50
23	15:21	.35-2.0	3.85	2.96	6.43
24	15:36	.35-1.3	3.98	3.04	6.18
25	15:51	.45-2.0	4.58	3.49	7.93
26	16:02	.35-2.0	4.18	2.84	5.51

Table 4. Characteristic values of spectra for Series B.

1	2	3	4	5	6
Run no.	Time of beginning	m (Range 0.55 Hz-3.0 Hz)	α (10^3 cm^{2}s)	u_* (cm s^{-1})	α_s (10^{-2})
1	12:51	3.95	1.45	23.3	6.37
2	12:52	4.28	1.31	24.6	5.43
3	12:53	4.24	1.28	23.8	5.49
4	12:54	4.15	1.26	22.8	5.64
5	12:55	4.18	1.19	19.2	6.30
6	12:56	4.04	1.38	17.2	8.17
7	12:57	4.18	1.35	19.7	6.98
8	12:58	4.12	1.40	19.6	7.30
9	12:59	4.13	1.51	19.0	8.13
10	13:00	4.21	1.43	17.5	8.35
11	13:01	4.05	1.62	17.9	9.22
12	13:02	4.19	1.43	20.2	7.22
13	13:03	4.11	1.37	21.9	6.39
14	13:04	4.03	1.47	25.0	6.01
15	13:05	4.03	1.52	28.7	5.39
16	13:06	3.77	1.86	27.5	6.88
17	13:07	3.91	1.72	28.5	6.15
18	13:08	4.05	1.73	24.4	7.24
19	13:09	4.20	1.73	25.4	6.95
20	13:10	4.43	1.57	26.1	6.13
21	13:11	4.21	1.85	32.0	5.88
22	13:12	4.08	1.90	34.9	5.55
23	13:13	4.07	1.89	34.7	5.55
24	13:14	4.23	1.73	33.2	5.33
25	13:15	4.22	1.85	30.8	6.11
26	13:16	4.07	1.96	30.3	6.60
27	13:17	4.08	1.82	30.8	6.03
28	13:18	3.95	2.06	33.0	6.38

computed with the method of least squares under the condition that the value of m was fixed to be 4. Computed values of α are shown in Column 5 of Table 3 and Column 4 of Table 4 for Series A and B, respectively. In Fig. 11 is shown the relation between α and u_*, where the values of u_* for Series B are 3-minute average values, which are listed in Column 5 of Table 4. It is concluded from the figure that α is proportional to u_*, and the formula (24) is satisfied. The values of α_s have then been computed and shown in Column 6 of Table 3 and Column 6 of Table 4 for Series A and B, respectively. The mean value of α_s with its standard deviation is

$$\alpha_s = 0.062 \pm 0.010 \qquad (29)$$

for Series A, and

$$\alpha_s = 0.065 \pm 0.010 \qquad (30)$$

for Series B. In Fig. 11 the line is drawn with the α_s value of Series A, since it contains a range of u_* wider than Series B.

In Fig. 12 is shown the power spectrum of Run 18 of Series A, as an example. In the figure, the solid line shows (24) with $\alpha_s = 0.062$ and the broken line shows (23) with $\alpha_p = 0.0074$. In Fig. 13 are shown power spectra of the first several runs of Series B, which have been extracted as examples from the entire figures drawn by an automatic drafter. The left part of the figure shows the power spectra normalized by (23) with $\alpha_p = 0.0074$, and the right part of the figure shows the power spectra normalized by (24) with $\alpha_s = 0.062$. It is seen from Figs. 12 and 13 that the $gu_*\sigma^{-4}$-form of wind wave spectra is in agreement with our present field data, except the range of higher frequencies than 3 Hz, apparently better than the Phillips' $g^2\sigma^{-5}$-form. The power spectra of the rest of the runs show almost the same tendency.

The two values of α_s shown by (29) and (30) for Series A and B are nearly the same with each other, but not equal to 0.020, that was proposed by TOBA (1973a) by use of his wind-

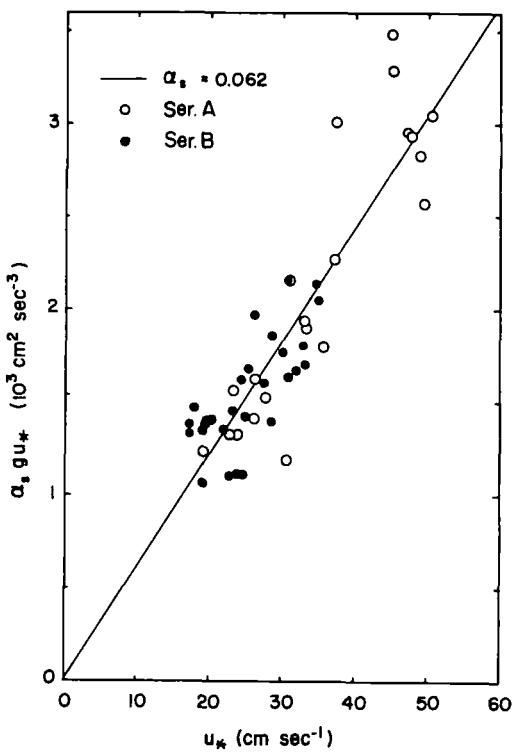

Fig. 11. Relation between α of Eq. (25) and u_*.

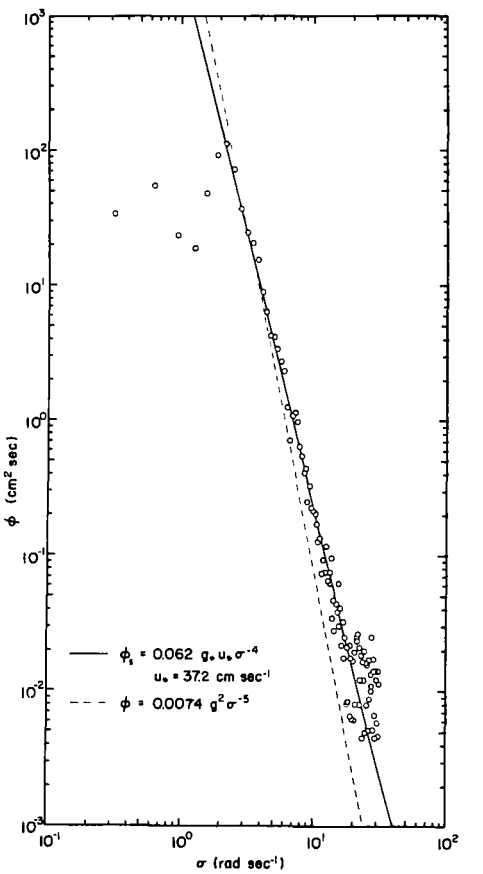

Fig. 12. An example of power spectrum for Run no. 18 of Series A.

wave tunnel data. The discrepancy is interpreted as follows. The spectra of wind waves in wind-wave tunnels are generally characterized by some zigzag pattern, which corresponds the phenomena of overshoot and undershoot. In the spectra of wind waves observed in the ocean, the zigzag pattern is less pronounced. This fact was noticed by TOBA (1973a) and also by RAMAMONJIARISOA (1973), and the situation is shown schematically in Fig. 14. TOBA (1973a)

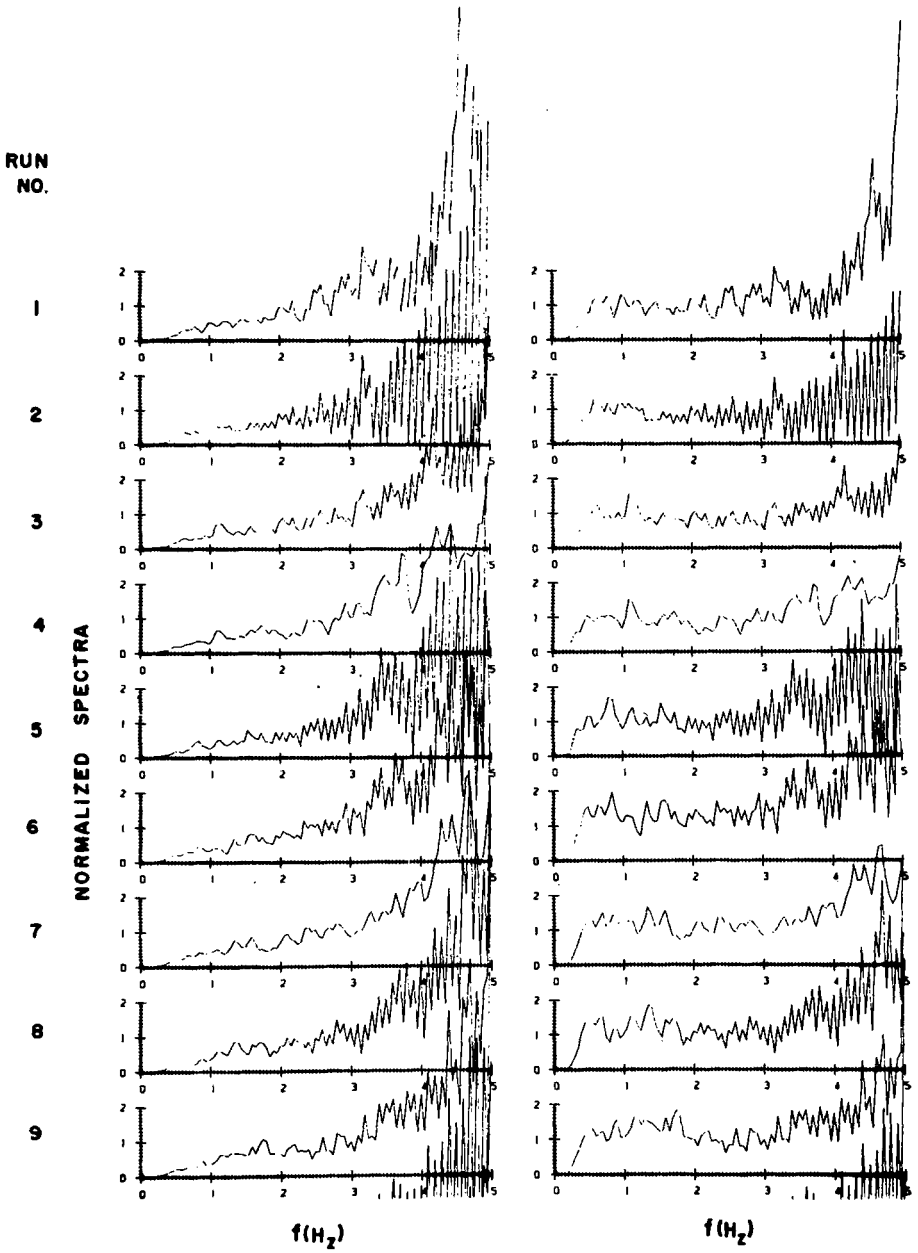

Fig. 13. Some examples of power spectra for Series B. Left; normalized by (23) with $\alpha_p=0.0074$. Right; normalized by (24) with $\alpha_s=0.062$. The values of the spectra for frequencies greater than 3 Hz is not significant, since, for this range, the accuracy in digitizing the record and the frequency response of the wave gauge will not be enough, and also there will be the folding effects. So, this part is not used in deciding α and m in (25).

proposed originally the form

$$\phi(\sigma)=\alpha_g g_* u_* \sigma^{-4} \qquad (31)$$

as the gross form representing the zigzag pattern on the $\log\phi$-$\log\sigma$ plot as shown in Fig. 14, and gave the value of α_g of 0.020. The α_s in (24) is distinguished from α_g in (31), where the subscript g stands for the gross form of the zigzag pattern. In order to compare the two types of the spectral pattern, or in order to compare α_s in (24) and α_g in (31), it is reasonable to consider the total energy of wind waves, or the integral of the spectrum. The Toba-Pierson spectral data (TOBA, 1973a) have been integrated over the frequency range greater than the spectral peak σ_m, and equivalent values of α_s have been obtained by use of the relation:

$$\int_{\sigma_m}^{\infty}\phi(\sigma)\,d\sigma=\int_{\sigma_m}^{\infty}\alpha_s g u_*\sigma^{-4}d\sigma \qquad (32)$$

where $\phi(\sigma)$ has a zigzag pattern. For twenty-one spectra, the mean value of α_s with its standard deviation is,

$$\alpha_s=0.056\pm0.011 \qquad (33)$$

in fairly well agreement with the value obtained in (29), when the values of standard deviation are taken into account. Thus the spectral form for very short fetches as observed in a wind-wave tunnel and that for long fetches as observed in the sea are represented consistently with (24), when the energy-level evaluation given by (32) is made for the zigzag pattern of the former. In other words, the spectral form for very short fetches transforms to that for long fetches, with the energy level α_s given by (32) conserved.

On the basis of these results, it seems necessary to reanalize old data of wave spectra. For example, a close inspection of Fig. 4.8 of PHILLIPS (1966) reveals that the σ^{-5}-line drawn in the figure represents an overall tendency of the summation of such individual data that have gradients near to σ^{-4}, as was already pointed out by TOBA (1973a). There are many literatures showing a similar situation. For example, wind-wave spectra shown in the paper by KONDO *et al.* (1973) are expressed very well by the formula (24) as shown in Fig. 15, except the higher frequency range of the case of $U_{10}=12.4$ m s^{-1}, although we do not conceive the cause of the deviation. In the figure circles and squares represent the original data, and

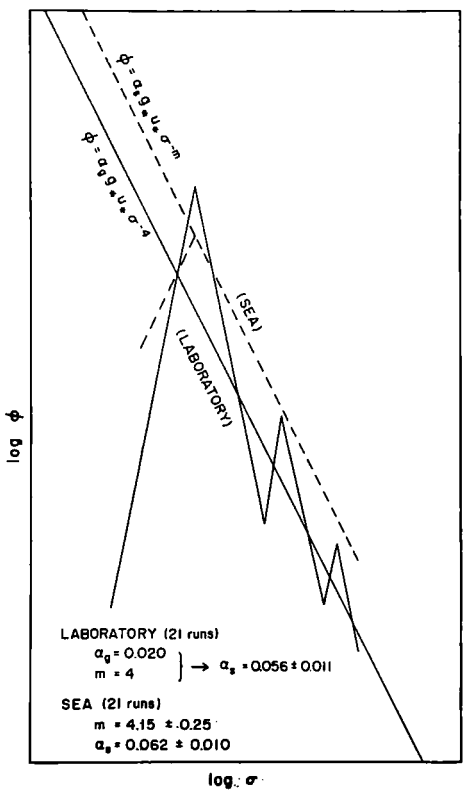

Fig. 14. A schematic pattern of wind wave spectra.

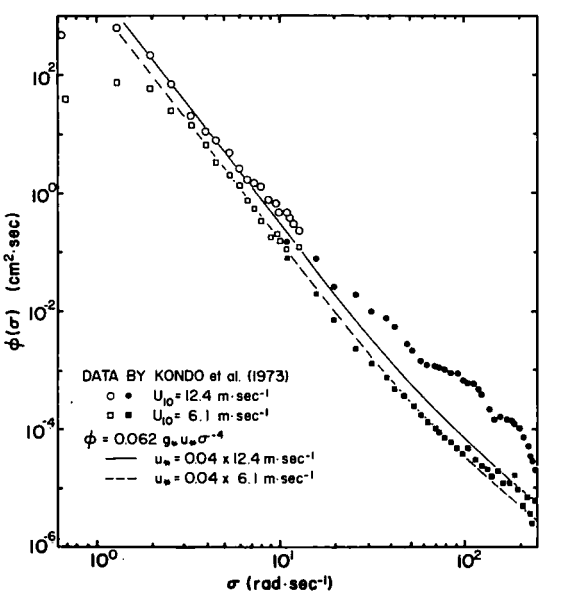

Fig. 15. The $gu_*\sigma^{-4}$-form and spectra observed by KONDO *et al.* (1973).

lines show the formula (24) with $\alpha_s=0.062$ and values of u_* computed from the values of U_{10} with $(C_D)^{1/2}=0.040$.

MITSUYASU and HONDA (1974) reported that their experimental data agrees with (24) in a general sense. MITSUYASU (1977) considers that there exists definitely the range represented by (24) with $\alpha_s=0.012$, but there also exists a range, nearer to the spectral maximum, represented by the $g^2\sigma^{-5}$-form. According to our opinion, wind wave field in the purely growing stage should be expressed by (24), and as soon as the wind becomes weak by the fluctuation of the wind, the effect of u_* drops and the spectral shape approaches to the $g^2\sigma^{-5}$-form, since the waves near the energy maximum decay slowly than the high frequency side. Consequently, actual wind wave spectra observed in the sea tend to have a form between (23) and (24), and since our present data represents the condition of approximately purely growing stage as described in the introduction, it has become a very good support to the wind wave spectral form of (24).

It should also be noted that TOBA (1976) has pointed out that JONSWAP composite data presented by HASSELMANN *et al.* (1976) may be interpreted as also giving a support to the $gu_*\sigma^{-4}$-form.

Acknowledgements

The authors express their deep thanks to the members of Kyoto University including Prof. H. KUNISHI, Messrs. K. NISHI, K. TANAKA, S. SERIZAWA, N. SHIBATA, Miss Y. SHIMADA and the late Mr. Y. SHIMIZU, who collaborated in the observation at the Shirahama Oceanographic Tower Station, Kyoto University, in November, 1969. Thanks are also due to Mr. M. TOKUDA of Tohoku University for discussing and making some computations about the significant waves. The computation contained in the present article was performed by use of NEAC-2200-700 at the Computer Center of Tohoku University. This study was partially supported by the Grant-in-Aid for Scientific Research, Project No. 942004, by the Ministry of Education.

References

HASSELMANN, K., T. P. BARNETT, E. BOUWS, H. CARLSON, D. E. CARTWRIGHT, K. ENKE, J. A. EWING, H. GIENAPP, D. E. HASSELMANN, P. KRUSEMAN, A. MEERBURG, P. MÜLLER, D. J. OLBERS, K. RICHTER, W. SELL and H. WALDEN (1973): Measurements of wind-wave growth and swell decay during the Joint North Sea Wave Project (JONSWAP), Deut. Hydrogr. Z., Suppl. A, **8**, No. 12, 1-95.

HASSELMANN, K., D. B. ROSS, P. MÜLLER and W. SELL (1976): A parametric wave prediction model. J. Phys. Oceanogr., **6**, 200-228.

HAYAMI, S., H. KUNISHI and K. NISHI (1964): On Shirahama Oceanographic Tower Station and some interesting records (in Japanese with English abstract). Ann. Disas. Prev. Res. Inst., Kyoto Univ., **7**, 434-458.

IWATA, N., W. INADA, T. TANAKA and I. WATABE (1970): Ocean wave statistics and spectrum width parameter (I) (in Japanese with English abstract). Rep. Natl. Res. Center for Disaster Prevention No. 4, 23-43.

IWATA, N., W. INADA and I. WATABE (1971): Ocean wave statistics and spectrum width parameter (II) (in Japanese with English abstract). Rep. Natl. Res. Center for Disaster Prevention No. 5, 81-87.

KONDO, J., Y. FUJINAWA and G. NAITO (1973): High-frequency components of ocean waves and their relation to the aerodynamic roughness. J. Phys. Oceanogr., **3**, 197-202.

LONGUET-HIGGINS, M. S. (1952): On the statistical distribution of the heights of sea waves. J. Mar. Res., **11**, 245-266.

MITSUYASU, H. (1968): On the growth of the spectrum of wind-generated waves (I). Rep. Res. Inst. Appl. Mech., Kyushu Univ., **16**, 459-482.

MITSUYASU, H. (1971): On the form of fetch-limited wave spectrum. Coastal Engineering in Japan, **14**, 7-14.

MITSUYASU, H. (1973): The one-dimensional wave spectra at limited fetch. Rep. Res. Inst. Appl. Mech., Kyushu Univ., **20**, 37-53.

MITSUYASU H. (1977): The measurement of high frequency spectrum of ocean surface waves. J. Phys. Oceanogr., **7**. (in press)

MITSUYASU, H., R. NAKAYAMA and T. KOMORI (1971): Observations of the wind and waves in Hakata Bay. Rep. Res. Inst. Appl. Mech., Kyushu Univ., **19**, 37-74.

MITSUYASU, H. and T. HONDA (1974): The high frequency spectrum of wind-generated waves. J. Oceanogr. Soc. Japan, **30**, 185-198.

MITSUYASU, H., F. TASAI, T. SUHARA, S. MIZUNO, M. OHKUSU, T. HONDA and K. RIKIISHI (1975): Observations of the directional spectrum of ocean waves using a cloverleaf buoy. J. Phys. Oceanogr.,

5, 750-760.

PHILLIPS, O.M. (1958): The equilibrium range in the spectrum of wind-generated waves. J. Fluid Mech., **4**, 426-434.

PHILLIPS, O. M. (1966): The Dynamics of the Upper Ocean. Cambridge Univ. Press, London, 261 pp.

PIERSON, W. J., JR. (1952): A unified mathematical theory for the analysis, propagation and refraction of storm-generated ocean surface waves, Parts I and II. N. Y. U., Coll. of Eng., Res. Div., Dept. of Meteorol. and Oceanogr. Prepared for the Beach Erosion Board, Dept. of the Army, and Office of Naval Res., Dept. of the Navy, 461 pp.

PIERSON, W. J., JR. and L. MOSKOWITZ (1964): A proposed spectral form for fully developed wind sea based on the similarity theory of S. A. KITAĬGORODSKIĬ. J. Geophys. Res., **69**, 5181-5190.

RAMAMONJIARISOA, A. (1973): Sur l'évolution des spectres d'énergie des vagues de vent a fetchs courts. Mém. Soc. Roy. Sci. de hiège, 6ª série, **6**, 47-66.

SVERDRUP, H.U. and W.H. MUNK (1947): Wind, sea and swell. Theory of relations for forecasting. U.S. Hydrogr. Office, Wash., Publ. No. 601, 1-44.

TOBA, Y. (1961): Drop production by bursting of air bubbles on the sea surface (III). Study by use of a wind flume. Memoirs, Coll. Sci., Univ. Kyoto, Ser. A. **29**, 313-344.

TOBA, Y. (1972): Local balance in the air-sea boundary processes, I. On the growth process of wind waves. J. Oceanogr. Soc. Japan, **28**, 109-120.

TOBA, Y. (1973): Local balance in the air-sea boundary processes, II. Partition of wind stress to waves and current. J. Oceanogr. Soc. Japan, **29**, 70-75.

TOBA, Y. (1973a): Local balance in the air-sea boundary processes, III. On the spectrum of wind waves. J. Oceanogr. Soc. Japan, **29**, 209-220.

TOBA, Y. (1974): Duality of turbulence and wave in wind waves. J. Oceanogr. Soc. Japan, **30**, 241-242.

TOBA, Y. (1974a): Macroscopic principles on the growth of wind waves. Sci. Rep. Tohoku Univ., Ser. 5, Geophys., **22**, 61-73.

TOBA, Y. (1976): Stochastic form of the growth of wind waves and its physical implications. Book of Abstracts, Joint Oceanographic Assembly, Edinburgh, 1976, p. 192.

TOBA, Y., H. KUNISHI, K. NISHI, S. KAWAI, Y. SHIMADA and N. SHIBATA (1971): Study of the air-sea boundary processes at the Shirahama Oceanographic Tower Station. Disaster Prevention Res. Inst., Kyoto Univ., Annals, **14B**, 519-531 (in Japanese with English abstract).

TOBA, Y., M. TOKUDA, K. OKUDA and S. KAWAI (1975): Forced convection accompanying wind waves. J. Oceanogr. Soc. Japan, **31**, 192-198.

WILSON, B. W. (1965): Numerical prediction of ocean waves in the North Atlantic for December, 1959. Deut. Hydrogr. Z., **18**, 114-130.

発達しつつある風波に関する3/2乗則とスペクトルの $gu_*\sigma^{-4}$ 形の観測資料による裏付け

河合三四郎*，岡田弘三**，鳥羽良明*

要旨：1969年11月に得られた京都大学白浜海洋観測塔における海面境界過程に関する観測資料を解析し，発達しつつある風波の場の構造を代表する例として提示する．観測は，理想的な陸向きの風の条件下で行なわれ，4高度の風速，風向，気温，水温，および風波について6時間以上の連続記録が得られている．解析結果の主要な結論は以下のとおりである．(1)風速および風の海面応力に，特徴的な約6分周期の変動があった．(2) $H^*=BT^{*3/2}$ と $\delta=2\pi BT^{*-1/2}$ で表わされる3/2乗則とその系に対して，この資料は非常によい裏付けとなる．ここに $H^*(\equiv gH/u_*^2)$ と $T^*(\equiv gT/u_*)$ はそれぞれ無次元の有義波の波高と周期であり，δ は波形勾配，u_* は空気の摩擦速度，g は重力加速度，そして $B=0.062$ は普遍定数である．(3)スペクトルピークの高周波側のスペクトル形は $\phi(\sigma)=\alpha_s g u_* \sigma^{-4}$ の形でよく表わされる．ここに σ は角周波数，$\phi(\sigma)$ はスペクトル密度である．α_s の値として，この観測資料から 0.062 ± 0.010 が得られた．風洞水槽で得られる風波のスペクトル形と海で得られるものとは，前者がスペクトルピークの顕著な高調波を含んでいる点で著しく異なる．その結果 α_s の値にも見かけ上差が存在する．しかし，この α_s の差は，高調波を含んだスペクトル形のエネルギーレベルを評価することによって解消される．

* 東北大学理学部地球物理学教室，〒980 仙台市荒巻字青葉

** 現宛先：日本気象協会東北本部，〒980 仙台市一番町2-1-2